Contemporary Mathematics
Volume 141, 1993

Hairy Little Legs: Feeding, Smelling, and Swimming At Low Reynolds Numbers

M.A.R. KOEHL

ABSTRACT. Many small organisms use appendages bearing arrays of hairs to capture food or molecules from the surrounding fluid, and to locomote through fluid or to move fluid past themselves. The performance of these appendages depends on how much of the fluid they encounter flows through the gaps between the hairs, rather than around the perimeter of the whole array. In this paper I discuss the interplay of experiment and theory as I review how biologists and mathematicians have worked together to explore the conditions under which an array of hairs slips through the fluid like a leaky sieve versus those under which it operates like a non-leaky paddle. We have employed approaches ranging from microcinematography of small aquatic animals and flow visualization around dynamically scaled physical models to calculations of velocity profiles between neighboring hairs. We have discovered conditions under which there is permission for morphological diversity of hairy appendages with little consequence to performance, versus conditions under which changes in behavior, size, or morphology can alter performance or lead to novel physical mechanisms of operation. Recent experiments have underscored the importance of the interactions of arrays of hairs with neighboring walls, such as the animal's body surface or the ground. In the past we have tended to lump all low-Reynolds-number phenomena together as creeping flow, but the studies reviewed here illustrate some striking transitions in function within this viscous-flow regime.

1991 *Mathematics Subject Classification.* Primary 76; Secondary 92.

The final version of this paper will be submitted for publication elsewhere. Supported by grants from the National Science Foundation (OCE-820134, and OCE-8917404 to M. Koehl; OCE-8117761 to G. Paffenhöfer, and OCE-9010115 to A. Cheer), the Office of Naval Research (N00014-90-J-1357 to M.A.R. Koehl), NASA Ames Research Center (NCC 2-626 to A. Cheer), and by a John Simon Guggenheim Memorial Foundation Fellowship and a John D. and Catherine T. MacArthur Foundation Fellowship Award to M. Koehl.

0271-4132/93 $1.00 + $.25 per page

1. Introduction

Many organisms use appendages bearing arrays of hairs to capture food or molecules from the surrounding fluid, or to locomote through the fluid or to move the fluid past themselves.

A wide variety of aquatic organisms from different phyla make their living by gathering particulate matter (e.g., single-celled algae, bacteria, organic particles) from the water around them (Ref. 1). Often the structures they use to capture the particles are made up of rows of cylinders. If these structures operate as filters, the flux of fluid through them determines the volume of water per unit time an organism can process, and the velocity gradients near individual hairs determine the efficiency of capture of paricles of various characteristics (Ref. 2). If, instead, these structures operate as raptorial appendages that actively capture individual food items, the amount of water "stuck to" and moving with an appendage determines whether an organism can reach out and grab a particle without pushing it away (Ref. 3).

Structures such as gills and antennae, which often bear arrays of hairs, are used to capture molecules rather than particles from the surrounding fluid. As with food capture, the flux of fluid through the array, as well as the steepness of the velocity gradients next to individual hairs, determines the rate at which molecules arrive at the surfaces of the hairs (e.g., Refs. 4, 5).

Many small animals use appendages bearing arrays of hairs to move through fluids, or to produce feeding or ventilatory currents past themselves (e.g., Refs. 3, 6, 7). The amount of fluid that leaks through the rows of hairs on such appendages rather than flowing around them should affect their ability to generate thrust and lift.

The names of these hairs and appendages are specific to particular organisms (e.g., "setules" on the "setae" of the "second maxillae" of calanoid copepods, "microtricia" on the "rays" of "antennae" of moths, or "asthetascs" on the "antennules" of lobsters), hence, for ease of discussion, I will avoid such jargon when I discuss the general case, and will simply refer to "hairs" or "bristles" on "appendages" or "legs."

The factors that determine the fluid motion through an array of cylinders is a significant basic biological question because so many different creatures use arrays of hairs in air or water to perform the variety of important functions listed above. The Reynolds number ($Re = UL/\nu$, where U is the velocity of the fluid relative to a hair, L is hair diameter, and ν is the kinematic viscosity of the fluid) at which these hairs operate is generally low (10^{-6} to 10; Refs. 2, 8); hence, viscous effects are important in determining flow patterns with respect to the hairs.

One of the purposes of this conference on biofluiddynamics is to bring together biologists and fluid dynamicists, and to enhance communication between experimentalists and theorists. Therefore, rather than simply discuss our latest research results on the fluid dynamics of hairy appendages, I will review

the interplay between experiment and theory in our past and ongoing work on how this commonly occurring type of appendage functions, and how its behavior and morphology affect performance. The leap-frogging between our empirical biological studies and mathematical modeling is diagrammed in Figure 1.

2. Filter-feeding theory

In spite of a wealth of information about the rates and ecological importance of filter feeding by various creatures, the mechanisms by which organisms capture particles from the surrounding water have been poorly understood. Biologists generally used to think that comb-like filter-feeding appendages were simply strainers that sieved particles larger than the gap between adjacent hairs out of the water passing through them. However, when Rubenstein and Koehl (Ref. 2) applied to biological filters the theoretical analyses of particle capture developed by engineers (reviewed in, e.g., Refs. 12–15), we pointed out that particles smaller than the gap-size could be captured by a variety of mechanisms other than sieving, including direct interception, inertial impaction, gravitational desposition, and motile-particle capture. By providing quantitative relationships between the intensity of particle capture by these various mechanisms and measurable parameters (such as paricle size and density, filter fiber diameter, and fluid velocity), engineering filtration theory suggested several biologically interesting predictions (Ref. 2). One was that filter feeders cannot help but capture some kinds of particles at greater rates than others; that is, simple physical processes render them "selective" feeders. Another was that an organism can, in theory, change the kinds of things it selectively captures by changing the velocity of the flow through its filter.

An oceanographer, T. Cowles, pointed out to me that some calanoid copepods can switch the selectivity of their particle capturing (Ref. 16), and convinced me that these ecologically important animals might provide a good system for testing some of the predictions of filtration theory.

3. Particle capture by calanoid copepods

Calanoid copepods are small (of the order of a few millimeters in body length) shrimp-like animals that can be extremely abundant in the water column of oceans and lakes. Many of these planktonic copepods feed on unicellular algae and other suspended particulate matter, forming a major link in many aquatic food webs. Because of the tremendous ecological importance of copepod feeding, many investigators have studied it, especially the rates at which copepods remove various kinds of particles from the water (reviewed in Ref. 11). In spite of all this attention, the mechanisms by which copepods capture particulate food were not understood; textbooks described a specific pair of appendages, the second maxillae (M2's) (Fig. 2), as filters that strained particles from a current of water forced through them by the beating of four other pairs of feeding legs (reviewed in Ref. 11).

The first step in analyzing the filtering by copepods was to work out the kinematics of their appendages during feeding, and to try to figure out the velocity of water flow through the filters (the M2's) when the animals captured particles of different sizes. Making such measurements posed a number of technical challenges: (1) a copepod is so small it must be viewed with a microscope, but the flow it creates cannot be studied if the animal is confined to a drop of water on a microscope slide, and (2) a copepod flaps its feet at high frequency, hence high-speed cinematography is necessary to resolve the leg motions. Fortunately, a technical breakthrough was made at the time that we needed kinematic data on feeding copepods: R. Strickler developed an optical system that permitted high-speed microcinematography of zooplankton in large containers of water (e.g., Ref. 17). By marking water near feeding animals with dye released from a micropipette, we were able to use Strickler's apparatus to work out the water and appendage motions during copepod feeding (Refs. 3, 10, 11, 18).

We discovered that the water current produced by the four pairs of feeding appendages by-passed the M2's (rather than flowing through the M2's as the literature had said). Our films of the copepod *Eucalanus pileatus* feeding on algaal cells (36 to 53 μm long) revealed that when a parcel of water containing a food particle neared a copepod, the animal actively drew that water and the particle toward its mouth by flinging the M2's apart (Fig. 3B). The animal then squeezed the M2's back together again, forming a cage around the particle, and pushed the captured particle into its mouth using a different pair of appendages. Movies of dye streams indicated that very little water flowed through *E. pileatus* M2's, and that particles were captured without touching the setae. However, films of dye streams near *E. pileatus* engaged in other behaviors (e.g., rejection of captured particles; Ref. 3), as well as later films of different species of copepods feeding on various types of particles (Koehl and Paffehöfer, unpublished data), revealed that in some cases water did flow through the M2's.

These observations that water sometimes does and sometimes does not flow through the M2's led us to table our original goal of using copepods to test some predictions of filtration theory, and to instead ask a more basic question: What determines how much fluid flows between the hairs in an array? Indeed, a debate soon grew in the biological literature about whether the hair-bearing appendages of a variety of planktonic animals operated as leaky sieves or as paddles (reviewed in Ref. 8).

4. Model of flow between a pair of hairs

What are the velocity profiles between adjacent hairs in a row? Although the case of an infinite row of cylinders of infinite length (in which all the fluid must pass through the gaps between cylinders) had been addressed (e.g., Ref. 19), the case of a finite row of hairs (in which fluid can pass both through and around the array), had not been explored at a range of gap-to-diameter ratios and Reynolds numbers that were biologically relevant. I turned to a theorist, A. Cheer, with

this question.

We first approached the problem by asking: How much fluid moves between a pair of infinitely long circular cylinders at low Reynolds numbers if the fluid is free to move around the hairs as well as between them? The calculations are described by Cheer and Koehl in Reference 8. Flow velocities near the hairs were calculated in bipolar coordinates by using Stoke's low-Reynolds-number approximation of the Navier-Stokes equations, and flow velocities far from the hairs were calculated in polar coordinates by using Oseen's low-Reynolds-number approximation (which takes inertial effects into consideration). A matched asymptotic expansion technique was used to put these two flow fields together (Ref. 20). We varied parameters such as velocity, diameter, and spacing of hairs over a biologically-relevant range.

Examples of velocity profiles calculated in this way are given in Figure 4A. These profiles can be used to calculate the "leakiness" of a pair of hairs, where leakiness is the ratio of the volume of fluid that actually flows through the gap in a unit of time to the volume that would have flowed through a space of that width if there were no hairs present. In Figure 4B, leakiness is plotted as a function of gap-to-diameter ratio for various Reynolds numbers. These calculations revealed several biologically-interesting phenonmena.

1. Is a hairy appendage a sieve or a paddle? As the Reynolds number increases, the leakiness increases. At Reynolds numbers approaching 1, little fluid is dragged along with the hairs as they move, and a hairy appendage should be sieve-like. In contrast, at very low Reynolds numbers, quite a bit of fluid is dragged along with the hairs and very little moves through the gap between adjacent hairs. Bristly appendages in this very-low-Reynolds-number range should behave more like solid paddles than like sieves.

2. What happens if an organism changes its Reynolds number, that is, its size or the speed of its motions? Such a change has very little effect on leakiness at very low Reynolds number ($\leq 10^{-3}$), hence there is great permission in this Reynolds number range for variation in size or behavior without consequences to the performance of functions that depend on appendage leakiness. In contrast, a change in Reynolds number in the range between 10^{-2} and 1 produces substantial change in leakiness, and hence in performance.

3. What happens to leakiness if the spacing between adjacent hairs is changed? At Reynolds numbers of 10^{-1} and 10^{-2}, there is a pronounced reduction in leakiness as hairs are moved closer together. At higher Reynolds numbers, this reduction in leakiness only occurs when the hairs are very close together, whereas at gap-to-diameter ratios greater than 15 there is no effect on leakiness of changing the spacing. At very low Reynolds numbers, there is also little effect on leakiness as a result of a change in gap width.

We tested this model by using it to calculate the leakiness of insect antennae for which empirical leakiness data were available. We also compared our results with predictions of leakiness of these antennae by using several other approaches

for estimating the flow through porous or fibrous structures. Our model predicted values closer to those measured for these antennae than did any of the alternative methods (Ref. 9).

5. Some biological implications of the model

Our model predicts effects on flow between cylinders due to differences in Reynolds numbers (i.e., size or speed) and the structure (i.e., gap-to-diameter ratio) of a hairy appendage. We can use these predictions to consider consequences of the changes in size, morphology, or behavior of such appendages that occur during the growth of an individual, or during the evolution of a lineage. Such changes should have little effect for microscopic organisms whose hairs operate at Reynolds numbers of 10^{-3} and lower, whereas at higher numbers (between 10^{-2} and 1), increases in Reynolds number or gap-to-diameter ratio can transform an appendage that was funtionally a paddle into a leaky sieve. Structures constrained to function as oars at small size acquire the potential to be filters at larger size. Conversely, if hairy appendages are to remain paddles when big, gaps between hairs should be very small (Fig. 4B) or should be filled in, for example, by membranes. Indeed, those insects and crustaceans that fly or swim with appendages made up of rows of hairs are quite small.

The same effects expected from an increase in size would also be expected from an increase in velocity. If an animal can alter the speed at which it moves an appendage, this plasticity in behavior should have leakiness consequences only for animals whose hairs operate in the Reynolds number range of 10^{-2} to 1.

Our suggestion that a novel function can accompany a simple change in the size or speed of a bristled structure of a small organisms may have evolutionary implications. Kingsolver and Koehl, studying the evolution of wings in insects, have demonstrated how an isometric change in the size of an animal can lead to a radically new function, and have suggested that this phenomenon might represent an important mechanism of evolutionary change (Ref. 21). If (as in the example of a hairy paddle becoming a filter) a structure acquires a novel function, it may well then be subjected to a new suite of selective pressures on its form.

6. Application of the model to copepod second maxillae

As mentioned above, water appears to flow through the second maxillae (M2's) of some species of copepods, but not of others. The morphology of the M2's varies from species to species, as illustrated in Figure 2. Each M2 bears a row of hairs (called setae), each of which bears rows of smaller hairs (called setules). The size of the setae, and the size and spacing of the setules depends on species, whereas the gaps between setae depend on how far an animal spreads its setae apart during a particular fling (Fig. 3B). The differences in speed of motion of the M2's is more striking than the differences in morphology between species (e.g., Ref. 3). The setae of copepod M2's operate at Reynolds numbers between

10^{-2} and 1 (Refs. 3, 10, 11), the range in which theory predicts that leakiness should be sensitive to Reynolds number and gap-to-diameter ratio.

We have used the model of Cheer and Koehl (Ref. 8) to calculate the leakiness of copepod M2's. The parameters used in these calculations were based on measurements for five species chosen to represent a range of morphologies and behaviors. Frame-by-frame analysis of high-speed movies of these copepods feeding on algal cells of various sizes yielded values for velocities and spacings of M2 setae (Koehl and Paffenhöfer, unpublished data). Morphometric analyses of light micrographs and scanning electron microscope images of the M2's of the animals filmed provided values for the diameters of setae and setules, and for setule lengths, spacings, and angles (Koehl, unpublished data).

The velocity profiles around a seta with a neighbor were calculated (Fig. 5A), and then the setules were placed at the appropriate angle in the flow field (Fig. 5B). Using the velocities thus calculated for free-stream velocities at defined positions on the setules, the velocity profiles between a pair of setules were calculated (Fig. 5C, and 5D). We then integrated across these velocity profiles to calculate leakiness of the second maxillae.

Figure 6 illustrates the leakiness of M2's from a species whose setae operate at Reynolds numbers approaching 1, *Centropages typicus* (Fig. 5C), and from a species whose setae operate at Reynolds numbers of the order of 10^{-2}, *Temora stylifera* (Fig. 5D). Note how much leakier the faster, coarser *C. typicus* M2 is. This example shows two copepods that superficially appear to be doing the same thing (both are a few millimeters long, both use hairy M2's to catch particles, and both move their M2's in qualitatively the same way – a fling outward and a squeeze back in); however, one of these species is about 50 times leakier than the other simply because it operates at a higher Reynolds number *in the critical range* where the Reynolds number makes a difference to leakiness.

Figure 6 illustrates another important difference between hairy appendages at these two ends of the critical range. When a hinged appendage flaps at some angular velocity, its distal end moves at a greater speed than does its proximal end. The Reynolds numbers along the length of a seta of an animal such as *C. typicus*, whose setal tips operate at Reynolds numbers near one, span the critical range where leakiness is sensitive to Reynolds number. Therefore, such an appendage is much leakier at its tip than at its base (unless its morphology is drastically different at base than tip). Note that this is not true for animals such as *T. stylifera*, whose M2 setal tips operate at Reynolds numbers of 10^{-2} or lower.

Does water move around the M2's of these species of copepods as theory predicts, and if so, what consequences do these differences in leakiness have for the mechanisms that variuos copepods can use to catch particles?

7. Particle capture by second maxillae at different Reynolds numbers

Theory predicts that M2's operating at Reynolds numbers near 1 should be leaky filters, whereas M2's operating at Reynolds numbers of 10^{-2} should be paddles. By looking at movies of fine dye lines in the water as copepod M2's sweep through them, we can see whether these predictions of the model are correct.

As predicted by the model, the M2's of *Centropages furcatus* and *C. typicus* are very leaky (Fig. 3C–3F). When a *Centropages* flings its M2's out, it does not disturb the fluid very much (note that the dye does not move between Figs. 3C and 3D). When the animal squeezes its M2's back in, water moves readily between the setae (as shown by the dye loops left behind between the setae as they sweep across the dye lines in Figs. 3E and 3F). Particles are filtered out of the water passing through the M2's during this squeeze phase of the motion (Koehl and Paffenhöfer, unpublished data).

In contrast, the M2's of species such as *T. stylifera* and *E. pileatus*, whose M2 setae operate at Reynolds numbers of 10^{-2}, are not very leaky (Figs. 3G, 3H) and behave like paddles, as predicted by theory. When these animals fling their M2's apart, a parcel of water (and any food particles in it) is drawn between them and toward the mouth, as described by Koehl and Strickler (Ref. 3). This flinging motion is reminiscent of that used by some insects to develop circulation around their wings (e.g., Refs. 22, 23). The M2's then squeeze back together again around the captured water, and the particle in that water is propelled to the mouth by the stubby endites of the first maxillae (Ref. 3).

These examples illustrate that different species of copepods that qualitatively do the same thing – fling and squeeze their M2's to catch an algal cell – can be capturing the cell by entirely different physical mechanisms because their M2's operate at different Reynolds numbers *in the critical range where leakiness changes with Reynolds number.*

8. Leakiness and changes in behavior

The model predicts that if an animal's hairs operate at Reynolds numbers in the critical range between 10^{-2} to 10^{-1}, then a change in the spacing between hairs or in the speed of motion can produce a change in leakiness. *E. pileatus* shows considerable plasticity in its M2 motions (e.g., Refs. 3, 24; also, Koehl and Paffenhöfer, unpublished data), and the setae of its M2's operate in this critical Reynolds number range.

Without getting into the details of all of *E. pileatus*'s varied behaviors and the circumstances in which it uses them, let us focus on the flow through the M2's during two extreme behaviors (Fig. 7). During a rejection of captured material, the fastest motion the M2 makes with its setae spread the greatest distance apart, the calculated leakiness at the distal end of the appendage is 31%. In contrast, when *E. pileatus* feed on very small algae (e.g., 4 μm) they do not fling

in response to individual cells, but rather pump a stream of water toward the mouth with a series of low-amplitude fling-and-squeeze motions. During these slow M2 motions, the gaps between setae are small and the calculated leakiness is only 14%. Hence, *E. pileatus* illustrates that an organism is not necessarily constrained by the morphology of its hairy appendages to just one leakiness: if it operates in the critical Reynolds number range, it can alter its leakiness by changing its behavior.

9. Calculation of velocity profiles around two and four cylinders at Reynolds numbers of order one

The analytical model described in Cheer and Koehl (Ref. 8) only deals with two cylinders at Reynolds numbers < 1, whereas most hairy appendages bear more than two hairs and some animals operate their hairs at Reynolds numbers > 1. Therefore, Cheer and Abdullah (unpublished text) used numerical calculations of steady, two-dimensional flow around infinitely long cylinders to investigate the consequences of adding more cylinders to a row and to explore the flow at Reynolds numbers of the order of 1. The numerical solution to the Navier-Stokes equations in vorticity stream-function formulation was obtained in generalized coordinates on a grid fitted to the geometry. The alternating direction implicit (ADI) method was used to solve the vorticity equations and the successive over-relaxation (SOR) method was used to solve the stream-function equations. Their results have intriguing biological implications.

Figure 8 illustrates Cheer and Abdullah's prediction of the consequences for a row of four cylinders of increasing Reynolds number from 0.5 to 4. Not only does leakiness increase as the Reynolds number rises, but the shapes of the velocity profiles become irregular, with velocity peaks near the cylinders. In contrast to lower Reynolds numbers, the velocities attained between the cylinders at Reynolds numbers > 1 exceed the free-stream velocity. As mentioned in the introduction, the steepness of the velocity gradients adjacent to the hairs of filter-feeding appendages or of appendages that capture molecules (gills, olfactory antennae) are important in determining the flux of particles or molecules to the capturing surfaces of the hairs. The calculations of Cheer and Abdullah point out that at Reynolds numbers of the order of 1, a small change in the speed of a row of hairs can make a big difference to the steepness of that velocity gradient. Empirical studies must be conducted to determine whether organisms take advantage of this physical phenomenon as they deploy their antennae, gills, and filters.

What happens to fluid motion if the number of hairs in a row is changed (by injury, during the development of an individual, or through the evolution of a lineage)? The velocities calculated by Cheer and Abdullah for two and four hairs are illustrated in Figure 9. At Reynolds numbers < 1, the addition of more hairs reduces leakiness, whereas at Reynolds numbers > 1, the addition of more hairs increases leakiness. We have here an example of a simple morphological change

that has *opposite* consequences at slightly different Reynolds numbers. Figure 9 also illustrates that the leakiness of a four-haired appendage is more sensitive to a change in Reynolds numbers than is the leakiness of two-haired appendage (i.e., the performance of the former is more sensitive to growth or behavioral change than is the performance of the latter).

Although these numerical calculations (Cheer and Abdullah, unpublished) permitted analysis of more hairs and higher Reynolds numbers than were possible with the model of Cheer and Koehl (Ref. 8), one row of four infinitely long hairs operating at steady state in an infinite fluid is still a far cry from a flapping pair of M2's. What other tools are available for studying the biofluiddynamics of such complicated structures?

10. Comparison of techniques for studying biofluiddynamics

Biofluiddynamical questions can be addressed using a variety of empirical and theoretical tools, each with different advantages and limitations.

1. We can measure the motions and forces of real organisms and the fluids around them, although all the technical challenges of doing so for rapidly moving microscopic creatures have not yet been solved. Unfortunately, exploration of the consequences of variations in morphology or behavior is limited by the diversity available in nature. Therefore, we cannot systematically vary one parameter at a time while holding all others constant to quantify the effects of each.

2. Mathematical models permit us to express quantitatively theories about the mechanisms underlying a process, or to describe quantitatively the behavior of a system. Such models enable us to predict the effects on performance of varying defined parameters, and they also permit us to study combinations of morphology and behavior not found in nature. However, with mathematical models, we are limited to relatively simple geometries and kinematics.

3. A third alternative is to measure forces or velocities of dynamically scaled physical models. Flow situations characterized by the same Reynolds numbers are dynamically similar (i.e., the ratios of the velocities and the forces at all points in the fluid around the model are the same as for the prototype). Therefore, a large model can be used to study the fluid dynamics of a microscopic structure if the model is moved slowly in a fluid of high viscosity to yield the same Reynolds number as that of the prototype. Repeatable, detailed velocity and force measurements that cannot be made on delicate, uncooperative microscopic organisms are technically possible with large models. Like mathematical models, dynamically scaled physical models have the advantage that parameters can be varied one at a time as the investigator chooses, and combinations that do not exist in nature can be tried. Such physical models, however, can be more complicated in geometry and behavior than is practical for mathematical models. Of course, as with mathematical models, physical models are only as good as their underlying assumptions.

11. Dynamically scaled models of pairs of cylinders

To use dynamically scaled models to explore the details of flow around rows of cylinders, I have joined forces with two other investigators who also need such information to study the capture of molecules by hairy olfactory appendages: B. A. Best, who is studying the olfactory antennules of crustaceans, and C. Loudon, who is studying the olfactory antennae of insects.

Before constructing more complicated models, our first exercise was to use such models to empirically test the predictions of Cheer and Koehl's model (Ref. 8). We used a computer-controlled RS-232, single-axis, microstepping servo-positioning system (Daedel rail table model 506301S-LH and controller model MC6000) to move a pair of steel cylinders through a 106-liter tank of Karo light corn syrup (CPC International). The cylinders were 1.98 mm in diameter and extended from the bottom of the tank through the top surface of the fluid (i.e., were "infinitely long"). Lines of small hydrogen bubbles generated hydrolytically (e.g., Refs. 25, 26) in the syrup were illuminated by a strobotac (GenRad model 1531-AB) flashing at known frequencies. Photographs were taken of the bubble paths relative to the cylinders by a 35-mm camera traveling with the wires. These photographs were digitized, and the velocity profiles measured between the cylinders were used to calculate leakiness.

These experiments with physical models are ongoing, and thus far we have only studied pairs of cylinders moving at Reynolds numbers of 10^{-2}, 10^{-3}, and 10^{-4}. Examples of our preliminary results for a pair of cylinders traveling parallel to the side wall of the tank are given in Figures 10 and 11. As predicted by theory (Ref. 8), we measured only slight changes in the steepness of the velocity gradients adjacent to cylinders with changes in Reynolds numbers at Reynolds numbers below the critical range. At these very low Reynolds numbers, we found that increasing the distance of the cylinders from the side wall decreased leakiness until the cylinders were 25 diameters from the wall; further increases in distance from the wall produced no measurable additional decrease in leakiness (Fig. 10). However, even in this plateau region, our measured leakinesses were greater than those calculated by Cheer and Koehl (Ref. 8) (Fig. 10), as were the steepnesses of velocity gradients near the cylinders (Fig. 11). Furthermore, the reductions in leakiness and in velocity gradient steepness produced by a decrease in the gap-to-diameter ratio were more pronounced than predicted by theory.

We believe that these discrepancies between theory and experiment are due to the effects of the tank walls and floor on the fluid motion with respect to the cylinders. Fluid sticks to the stationary boundaries of the tank and is sheared as objects move through the tank; therefore, at low Reynolds numbers where viscous effects dominate the flow, more fluid should be drawn through the gaps between cylinders traveling with respect to the walls than through the gaps between hairs moving in an unbounded fluid. Although we are not aware of analyses of wall effects at low Reynolds numbers on the flow between pairs of cylinders, studies of the effects of walls on spheres moving at low Reynolds numbers (e.g., Refs.

27, 28), and of the interactions of bodies near walls at low Reynolds numbers (e.g., Ref. 29), show that walls influence the flow around the bodies even when the bodies are hundreds of diameters from the wall. Of course, as we move to Reynolds numbers higher than 10^{-2}, we expect the effects of the wall to become less important (i.e., felt only at shorter distances, measured in cylinder diameters, from the wall).

It should not be surprising that the leakiness is further increased when the hairs move toward a front wall (Loudon, Best, and Koehl, unpublished data), analogous to an animal flapping an appendage toward the body surface. It should also not be surprising that leakiness is reduced if the hairs are of finite length (Best, Loudon, and Koehl, unpublished data), since fluid can flow around the tips of the hairs as well as around the sides of the row.

These experiments, rather than being useless because of wall effects, point out the importance of incorporating these effects into our models of low-Reynolds-number flow around appendages that operate near walls (e.g., the surface of the organism's body, other appendages, and the substratum in the case of terrestrial or benthic creatures). When hairy appendages flap near the body surfaces of organisms, they are likely to be leakier than they would be in an infinite fluid. Leakiness might vary with stage during a stroke as an appendage's distance from the body changes, and proximity to the body surface might compensate for the lower leakiness near the slowly moving base of an appendage (discussed above). Another important effect of walls that we have not yet studied is the consequences of a wall moving with the hairs (such as the appendage itself bearing the hairs, or as a moving organism bearing a non-flapping antenna). Wall effects in these cases should reduce the leakiness.

12. Comparison of theoretical results with measurements on second maxillae

Our measurements of flow between pairs of cylinders led me to worry about the effects of copepod body surfaces on the flow through M2's. I expected that leakiness calculated using the model of Cheer and Koehl (Ref. 8) would be lower than that measured for M2's whose setae operate at Reynolds numbers of 10^{-2}, but that the discrepancy would be minor at a Reynolds number of 1. I have begun to estimate leakiness of real M2's by measuring on our movies the dye loops left behind as setae sweep through them (as in Fig 3D). As shown by the preliminary data in Table 1, these estimates are the same as the leakinesses predicted by the model of Cheer and Koehl (Ref. 8) at Reynolds numbers near 1, but are about twice as big as predicted values at Reynolds numbers of the order of 10^{-2}.

13. Dynamically scaled physical models of second maxillae

We are using dynamically scaled physical models to explore more systematically the effects of the body surface and of other appendages on the flow around

copepod M2's. We have constructed models of the M2's of several species of copepods, and a motor-driven system that causes them to fling and squeeze at defined Reynolds numbers (in a 1000-liter tank of mineral oil at 470 diameters from the nearest wall). These models have realistic numbers of setule-bearing setae of finite length, and the motion of neutrally buoyant marker particles in the fluid around these structures can be filmed as they execute fling-and-squeeze motions in neighborhoods of various geometries. With these physical models it is possible to investigate geometries too complicated to be practical to model mathematically. For example, we can measure the effect on fluid flow of an M2 executing a fling-and-squeeze alone versus in opposition to the other M2 of a pair, of the distance between those paired appendages, of the arcs of the fling, and of the shape and proximity of the surface of the animals' body (Koehl and Jed, unpublished data).

14. Summary

Do hairy little legs function as paddles or as leaky rakes? Many organisms use appendages composed of small hairs to conduct a variety of important functions, such as capturing food or molecules, or locomoting through fluids. The performance of these functions depends on the velocity profiles of fluid moving through the array of hairs. We have studied factors that affect the flow through such arrays of hairs that operate at low Reynolds numbers.

1. Leakiness depends on Reynolds numbers: at Reynolds numbers of the order of 10^{-2} and lower, rows of hairs function like paddles, whereas at Reynolds numbers approaching 1, they behave like leaky sieves.

2. At Reynolds numbers $\leq 10^{-3}$, changes in morphology or Reynolds number have little effect on the leakiness between hairs. In this Reynolds number range, there is tremendous permission for morphological or behavioral diversity without performance consequences.

3. At Reynolds numbers $\geq 10^{-2}$, reducing the gap width between hairs reduces leakiness, although at Reynolds numbers approaching 1, this effect only occurs if hairs are already close together.

4. In the Reynolds number range of 10^{-2} to 1, increasing speed or size can lead to a large increase in leakiness. This is a critical range where morphology and behavior can have a big effect on the performance of functions that depend on velocity profile or leakiness. Novel functions (e.g., filtering) are possible without requiring the invention of novel morphologies.

5. At Reynolds numbers < 1, an increase in the number of hairs in a row reduces leakiness, whereas at Reynolds numbers > 1, an increase in the number of hairs leads to an increase in leakiness. Thus, a given morphological change can have *opposite* effects at different Reynolds numbers.

6. At low Reynolds numbers, the leakiness of an array of hairs is increased if the array moves with respect to a stationary wall. This effect is likely to be important for hairy appendages flapping at low Reynolds numbers with respect

to the body surface of an organism.

Biofluiddynamics is a field with a history of fruitful interaction between mathematical modelers and experimental scientists. In the example described in this paper, we set out to use copepod second maxillae to test some of the predictions of theoretical analyses of filters. Our empirical results showing that M2's were leaky enough to be filters only some of the time led us to explore another question: under what circumstances do rows of of hairs function as filters rather than as paddles? Mathematical models predicted the transition to occur as Reynolds number increases between 10^{-2} and 1. Experiments with dynamically scaled physical models (to permit us to study situations too complicated to be practical for mathematical modeling) pointed out the increase in leakiness caused by wall effects at low Reynolds numbers. These experiments led us to discover that the leakiness predicted by our mathematical models was lower than the values measured for real copepods whose setae operated at Reynolds numbers of 10^{-2}, but was the same as values measured for setae at Reynolds numbers near 1. These observations stimulated us to begin experiments with dynamically scaled models to study wall effects on the leakiness of paired flapping appendages. Thus, theory suggested experiments, whose results led to the formulation of new theory, and so on, as we leap-frogged our way between mathematical modeling and empirical studies toward a better understanding of the functioning of hairy appendages.

Acknowledgments

I am grateful to my collaborators D. Abdullah, A. Cheer, B. Best, T. Cowles, C. Loudon, G. Paffenhöfer, D. Rubenstein, and R. Strickler for their insights and technical expertise that made this work possible. I thank J. Ahouse, F. Dardis, P. Huie, J. Jed, S. Kahane, B. Okamura, M. Piccolo, and L. Sutanto for their technical assistance.

References

1. Jørgenson, C.B.: Biology of Suspension Feeding. Pergamon, Oxford, 1966.
2. Rubenstein, D.I.; and Koehl, M.A.R.: The Mechanisms of Filter Feeding: Some Theoretical Considerations. Amer. Narur., vol. 111, 1977, pp. 981–994.
3. Koehl, M.A.R.; and Strickler, J.R.: Copepod Feeding Currents: Food Capture at Low Reynolds Number. Limnol. Oceanogr., vol. 26, 1981, pp. 1062–1073.
4. Berg, H.C.; and Purcell, E.M.: The Physics of Chemoreception. Biophys. J., vol. 20, 1977, pp. 193–219.
5. Murray, J.D.: Reduction in Dimensionability in Diffusion Processes: Antenna Receptors of Moths. Nonlinear Differential Equation Models in Biology, University Press, Oxford, 1977, pp. 83–127.
6. Ellington, C.P.: Nonsteady-State Aerodynamics of the Flight of *Encarsia formoso*. Swimming and Flying in Nature, T.Y.-T. Wu et al., eds., vol. 2, Plenum, New York, 1975, pp. 783–796.
7. Barnes, R.D.: Invertebrate Zoology Fifth Ed. Saunders College Publishing, Philadelphia, 1987.
8. Cheer, A.Y.L.; and Koehl, M.A.R.: Paddles and Rakes: Fluid Flow through Bristled Appendages of Small Organisms. J. Theor. Biol., vol. 129, 1987, pp. 185–199.

9. Cheer, A.Y.L.; and Koehl, M.A.R.: Fluid Flow through Filtering Appendages of Insects. I.M.A. J. Math. Appl. Med. Biol., vol. 4, 1987, pp. 185–199.
10. Koehl, M.A.R.: Feeding at Low Reynolds Number by Copepods. Lect. Math. Life Sci., vol. 14, 1981, pp. 89–117.
11. Koehl, M.A.R.: Mechanisms of Particle Capture by Copepods at Low Reynolds Numbers: Possible Modes of Selective Feeding. Trophic Interactions in Aquatic Ecosystems, A.A.A.S. Selected Symposium No. 85, D.L. Meyers and J.R. Strickler, eds., Westview Press, Boulder, Colo., pp. 135–166.
12. Fuchs, N.A.: The Mechanics of Aerosols. Oxford, 1964.
13. Pich, J.: Theory of Aerosol Filtration by Fibrous and Membrane Filters. Aerosol Science, C.N. Davies, ed., Academic Press, New York, 1966, pp. 223–285.
14. Davies, C.N.: Air Filtration. Academic Press, New York, 1975, pp. 783–796.
15. Spielman, L.A.: Particle Capture from Low-Speed Laminar Flows. Ann. Rev. Fluid Mech., vol. 9, 1977, pp. 297–319.
16. Cowles, T.J.: The Feeding Responses of Copepods from the Peru Upwelling System: Food Size Selection. J. Mar. Res., vol. 37, 1979, pp. 601–622.
17. Alcarez, M.; Paffenhöfer, G.-A.; and Strickler, J.R.: Catching the Algae: A First Account of Visual Observations on Filter-Feeding Calanoids. Evolution and Ecology of Zooplankton Communities, W.C. Kerfoot, ed., University Press of New England, Hanover, N.H., 1980, pp. 241–248.
18. Koehl, M.A.R.: The Morphology and Performance of Suspension-Feeding Appendages. J. Theor. Biol., vol. 105, 1983, pp. 1–11.
19. Tamada, K.; and Fujikawa, H.: The Steady Two-Dimensional Flow of Viscous Fluid at Low Reynolds Numbers Passing through an Infinite Row of Equal Parallel Circular Cylinders. Quart. J. Mech. Applied Math., vol. 10, 1957, pp. 425–432.
20. Umemura, A.: Matched-Asymptotic Analyses of Low Reynolds Flow Past Two Equal Circular Cylinders. J. Fluid Mech., vol. 121, 1982, pp. 345–363.
21. Kingsolver, J.G.; and Koehl, M.A.R.: Aerodynamics, Thermoregulation, and the Evolution of Insect Wings: Differential Scaling and Evolutionary Change. Evolution, vol. 39, 1985, pp. 488–504.
22. Weihs-Fogh, T.: Quick Estimates of Flight Fitness in Hovering Animals. J. Exp. Biol., vol. 59, 1973, pp. 169–230.
23. Ellington, C.P.: Vortices and Hovering Flight. Proceedings of a Conference on Unsteady Effects of Oscillating Animal Wings, W. Nactigall, ed., Franz Steiner Verlag, Wiesbaden, 1980, pp. 64–101.
24. Price, H.J.; and Paffenhöfer, G.-A.; and Strickler, J.R.: Modes of Cell Capture in Calanoid Copepods. Limnol. Oceanogr., vol. 28, 1983, pp. 116–123.
25. Schraub, F.A.; Kline, J.; Henry, J.; Runstadler, P.W., Jr.; and Little, A.: Use of Hydrogen Bubbles for Quantitative Determination of Time-Dependent Velocity Fields in Low-Speed Flows. J. Basic Engin., Trans. A.S.M.E. Ser. D., 1965, pp. 429–444.
26. Roos, F.W.; and Willmarth, W.W.: Hydrogen Bubble Flow Visualization at Low Reynolds Numbers. AIAA J., vol. 7, 1969, pp. 1635–1637.
27. Happel, J.; and Brenner, H.: Low Reynolds Number Hydrodynamics. Prentice Hall, Englewood Cliffs, N.J., 1965.
28. White, F.M.: Viscous Fluid Flow. McGraw-Hill, N.Y., 1974.
29. Weinbaum, S.: Strong Interaction Theory for Particle Motion through Pores and near Boundaries in Biological Flows at Low Reynolds Number. Lect. Math. Life Sci., vol 14, 1981, pp. 119–192.

DEPARTMENT OF INTEGRATIVE BIOLOGY, UNIVERSITY OF CALIFORNIA, BERKELEY, CALIFORNIA 94720.

Table 1. Comparison of Measured and Calculated Leakiness

	Leakiness, %	
Species	Calculated[a]	Measured
Centropages furcatus (Reynolds number ~ 1)	92 to 96	95 S.D. = 3, $n = 4$
Eucalanus pileatus (Reynolds number ~ 10^{-2})	11 to 15	23 S.D. = 6, $n = 3$

[a] Calculated using the model of Cheer and Koehl (Ref. 8).

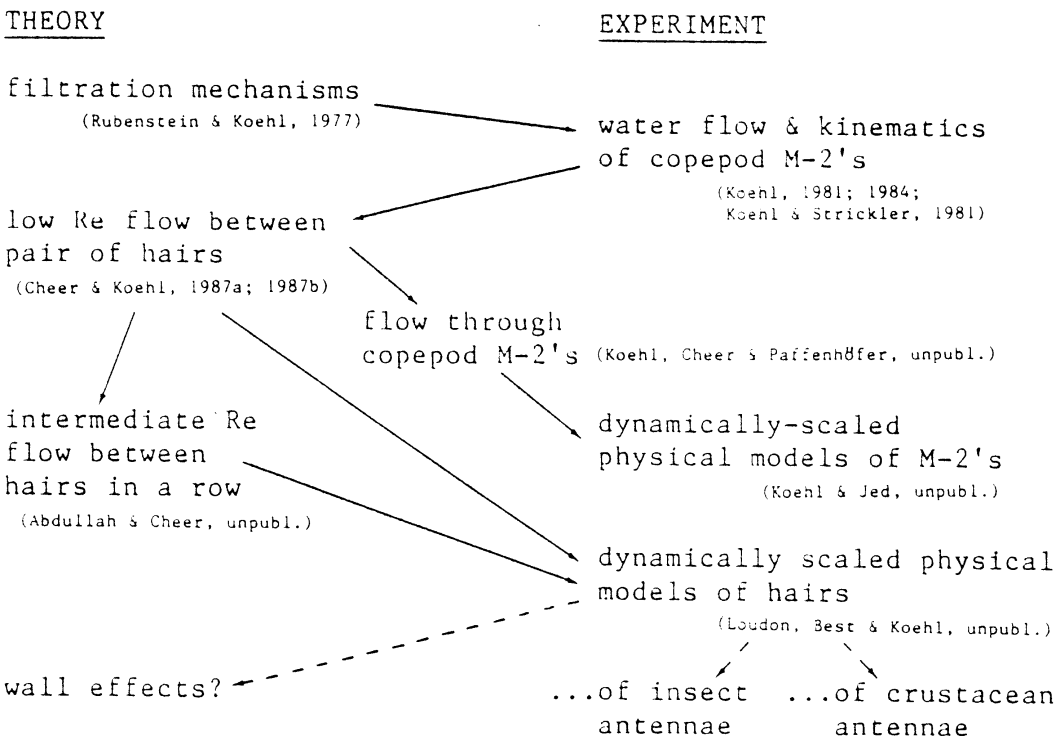

FIGURE 1. Flow chart illustrating interplay between theory and experiment in the investigation of biofluiddynamics of hairy legs. Solid arrows indicate which studies led to others; dashed arrows indicate studies to be conducted next.

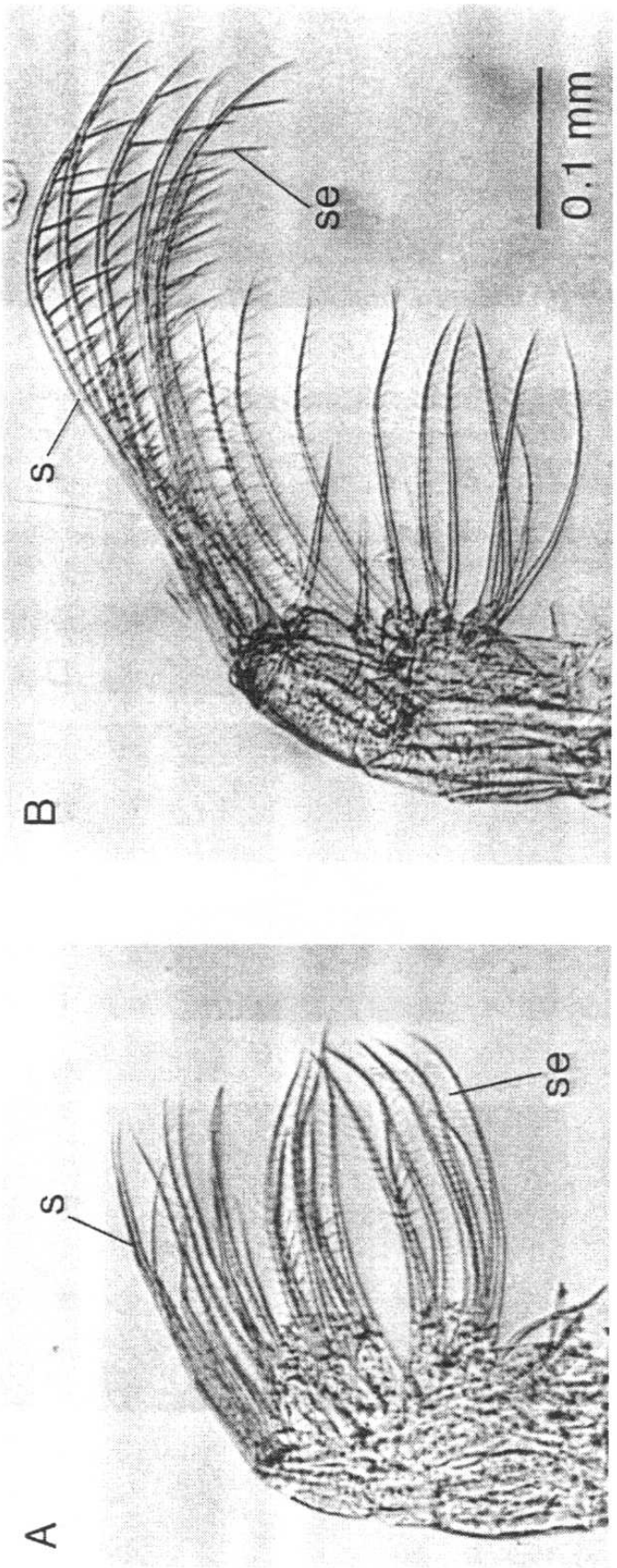

FIGURE 2. Second maxillae (M2's) of calanoid copepods, showing hairs (setae, "s") and smaller hairs they bear (setules, "se"). (A) *Temora stylifera*. (B) *Centropages furcatus*.

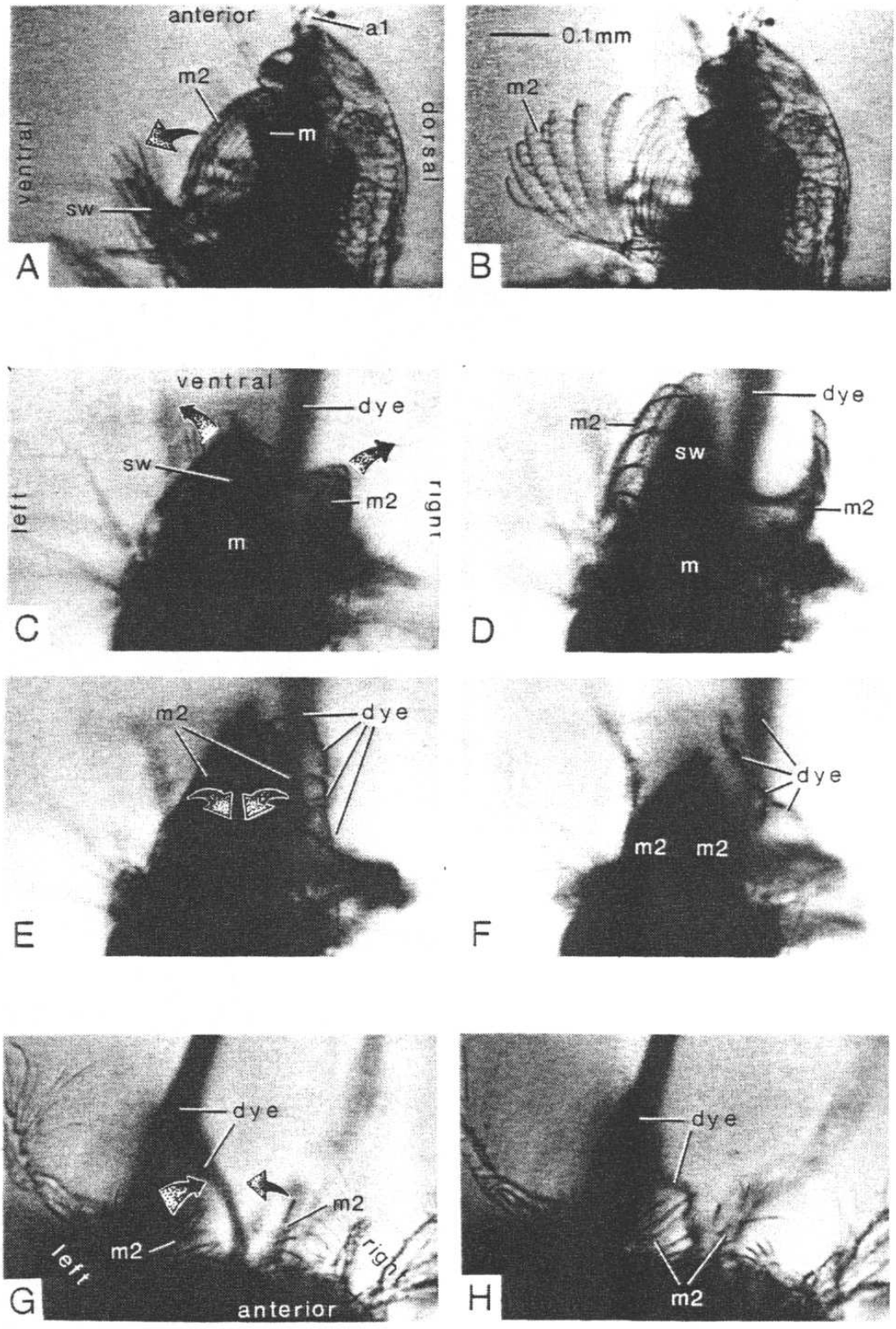
anterior
a1
m2
m
ventral
dorsal
sw
A
0.1mm
m2
B
ventral
dye
sw
m2
left
right
m
C
dye
m2
sw
m2
m
D
m2
dye
E
dye
m2
m2
F
dye
m2
left
m2
right
G
anterior
dye
m2
H

FIGURE 3. Photographs of single frames of high-speed (500 frames/sec) movies of calanoid copepods feeding on algal cells: m2 = second maxillae, m = mouth, a1 = first antenna, sw = swimming legs, dye = food coloring mixed with sea water and released from a micropipette 5 mm from animal. Arrows indicate direction second maxillae are moving. (A) Anterior half of a *Centropages furcatus* viewed from its left side as the M2's begin to fling. (B) Same animal 4 msec later, with the M2's flung apart. (C) *C. furcatus* viewed from its anterior end as the M2's are beginning to fling. (D) Same animal 2 msec later, with the M2's flung apart. (E) Same animal 2 msec later than in (D) as the M2's are squeezing back together. (F) Same animal 6 msec later than in (E), with the squeeze by the M2's completed. Note in (D) and (E) the loops of dye left behind marking water that has flowed between the setae during the squeeze. (G) Ventral portion of anterior end of a *Eucalanus pileatus* as seen in three-quarter view from its left anterior end while its M2's execute a squeeze. (H) Same animal as in (G) 4 msec later. Note how dye is pushed along by the setae and does not flow between the gaps.

(A)

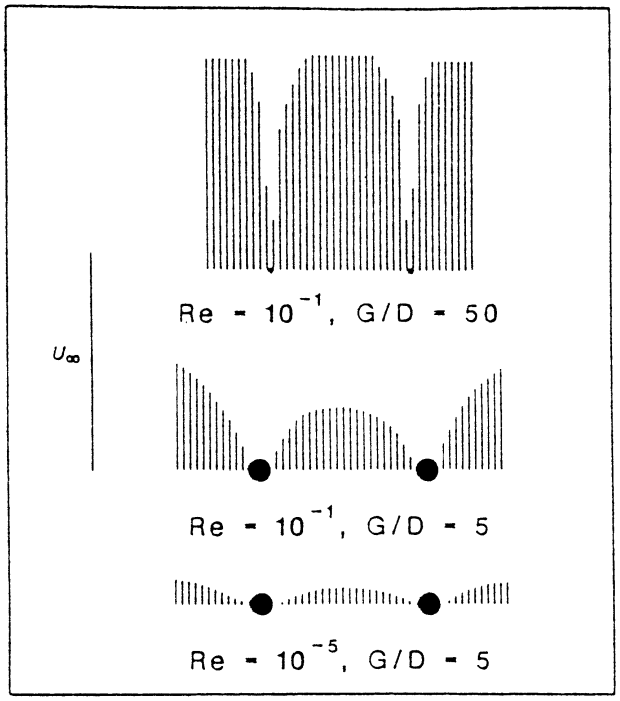

Reprinted with permission from "Paddles and rakes: Fluid flow through bristled appendages of small organisms" by A.Y.L. Cheer and M.A.R. Koehl, *J. Theor. Biol.* **129**, pp. 17–39, Figure 1.

(B)

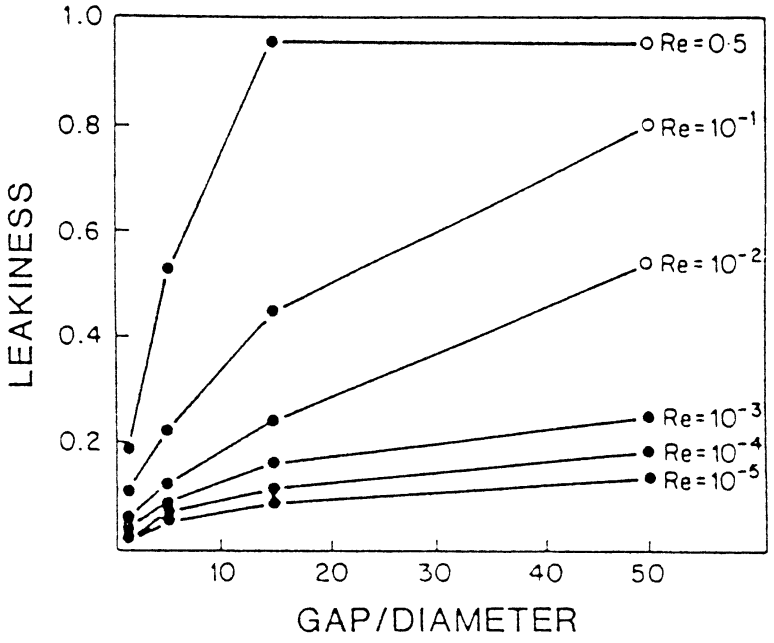

Reprinted with permission from "Paddles and rakes: Fluid flow through bristled appendages of small organisms" by A.Y.L. Cheer and M.A.R. Koehl, *J. Theor. Biol.* **129**, pp. 17–39, Figure 5.

FIGURE 4. (A) Examples of calculated fluid velocities (black lines) with respect to a pair of circular cylinders (black circles). Note that vectors are all drawn to the same scale with respect to free-stream velocity (U_∞, shown by the line to left of figure), although U_∞'s in each example are quite different from each other (redrawn from Fig. 1 in Ref. 8). (B) Leakiness (defined in the text) of a pair of cylinders plotted versus ratio of width of gap between cylinders to diameter of a cylinder. Flow profiles used for points indicated by open circles were calculated using Lamb's solution for Oseen's approximation to the Navier-Stokes equations of motion; flow profiles used for points indicated by black circles were calculated as described in text (redrawn from Fig. 5 in Ref. 8).

(A)

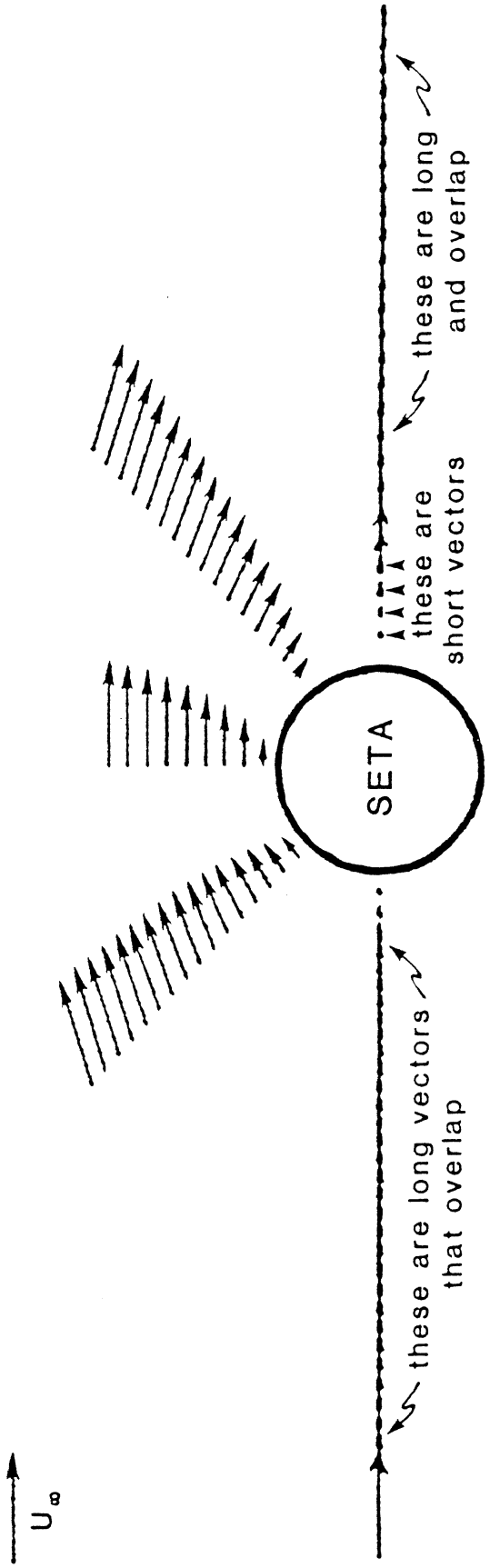
these are long
and overlap
these are
short vectors
SETA
these are long vectors
that overlap
U∞

(B)

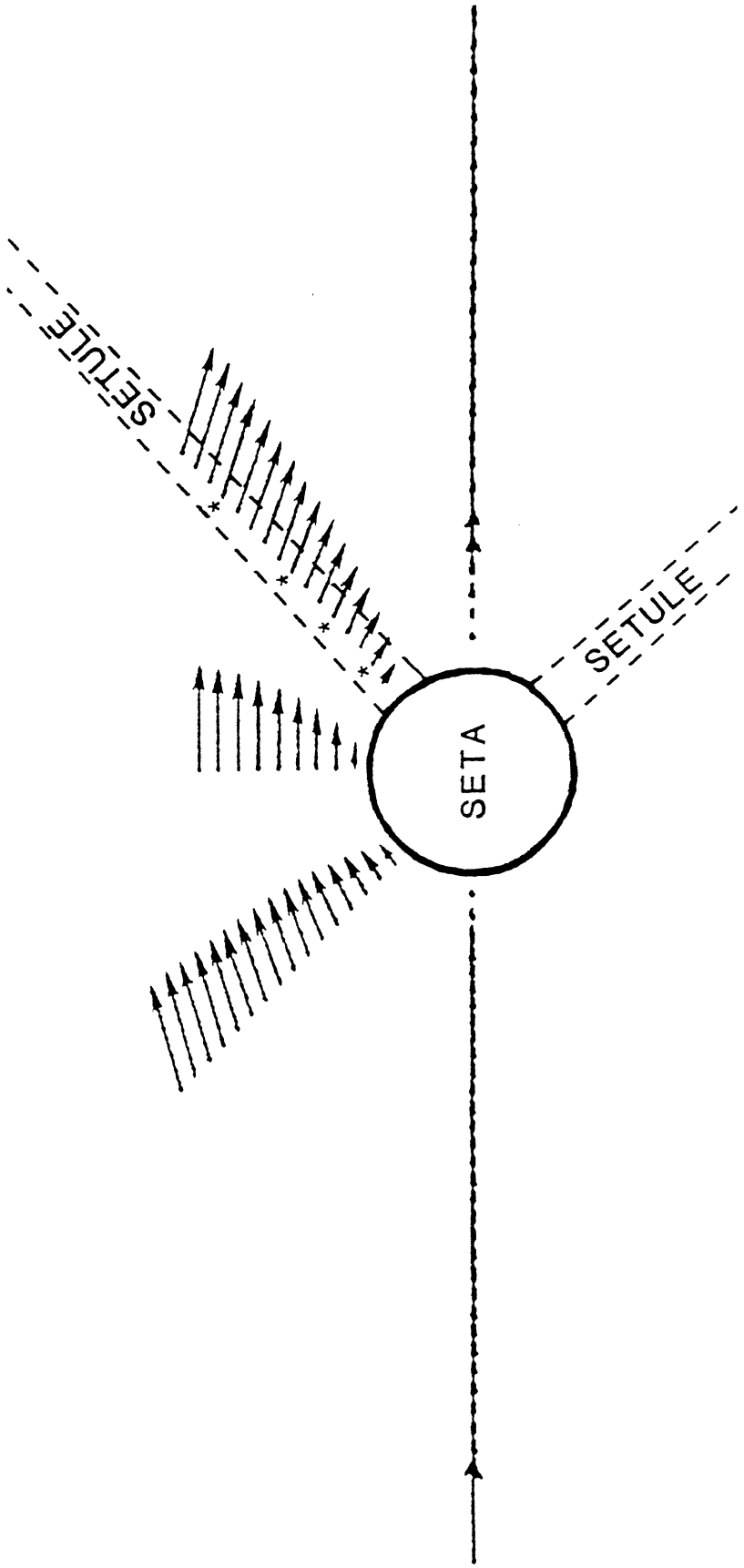

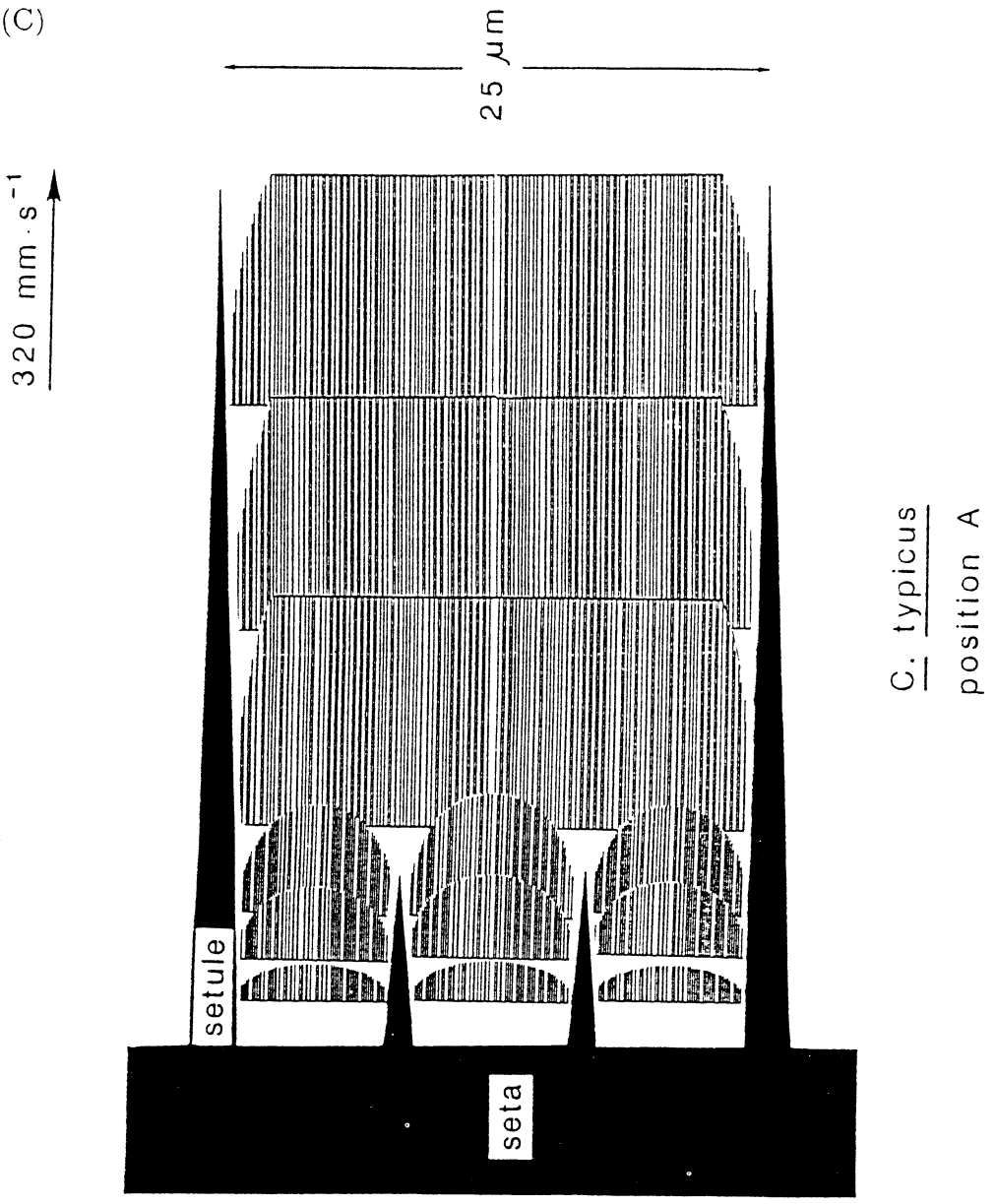
(C)
25 µm
320 mm·s⁻¹
setule
seta
C. typicus
position A

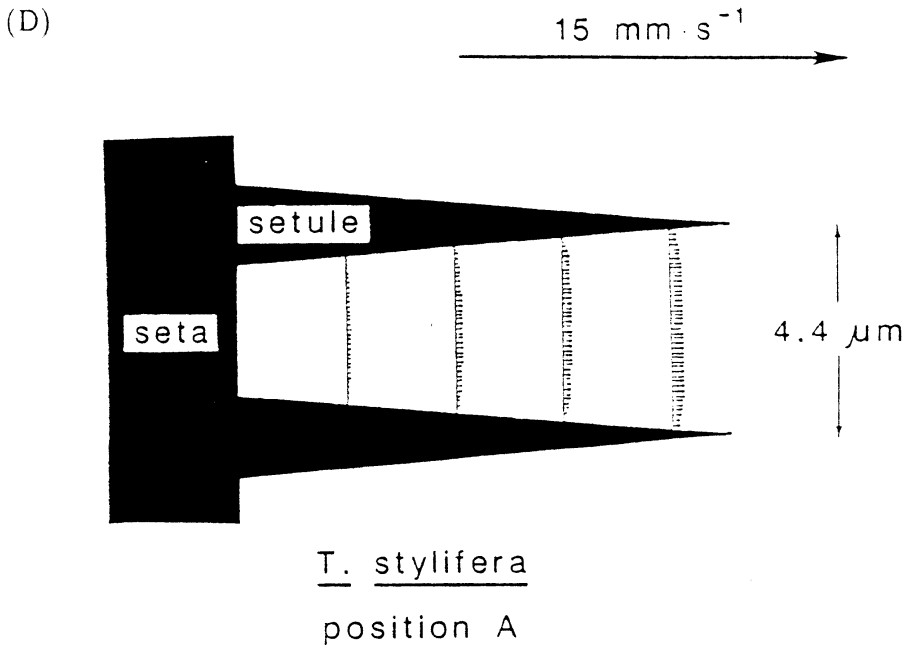

FIGURE 5. (A) Cross-section of a seta on the M2 of a *Centropages typicus* during a "fling," showing velocity vectors (arrows) of water with respect to the seta (calculated using model of Ref. 8). This seta, which bears no setules, is shown at a position 0.125 of the length of seta from the tip of seta. Free-stream velocity (U_∞) with respect to seta is indicated by arrow at upper left. (B) Position of setules (indicated by dashed lines) in the velocity profiles indicated in (A). Asterisks indicate positions at which velocity profiles with respect to setules were then calculated. The velocity vector shown here at each of these positions was used as the free-stream velocity encountered by that position. (C) Longitudinal section of a portion of the seta shown in (B), taken in a plane parallel to one of the two rows of setules (*C. typicus* M2's bear long and short setules). Lines represent velocity vectors of water with respect to setules, but at right angles to plane of diagram. Free-stream velocity with respect to the seta at right angles to plane of the diagram is indicated by arrow at the upper right. A vector shorter than this arrow indicates that some water at the position of the vector is moved along with the M2 as it flings. (D) Diagram as in (C) of the velocity vectors of water with respect to the setules of a *Temora stylifera* during a fling at a position 0.125 of the length of seta from tip of seta. Note that both size and velocity scales are different from those used in (C).

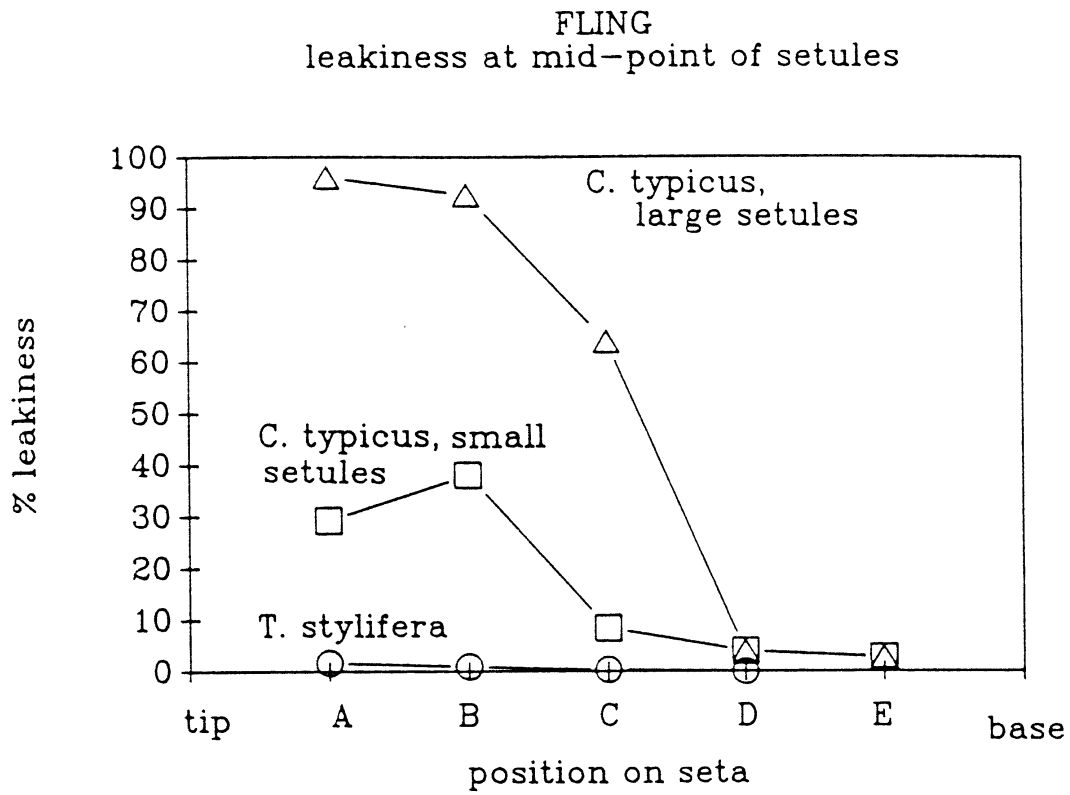

FIGURE 6. Leakiness calculated as described in text from velocity profiles at the midpoint along the length of setule at various positions along length of a seta. Positions A–E are evenly spaced along length of seta at intervals of 0.125 of length of seta. (Velocity profiles shown in Figs. 5C and 5D are for position A.)

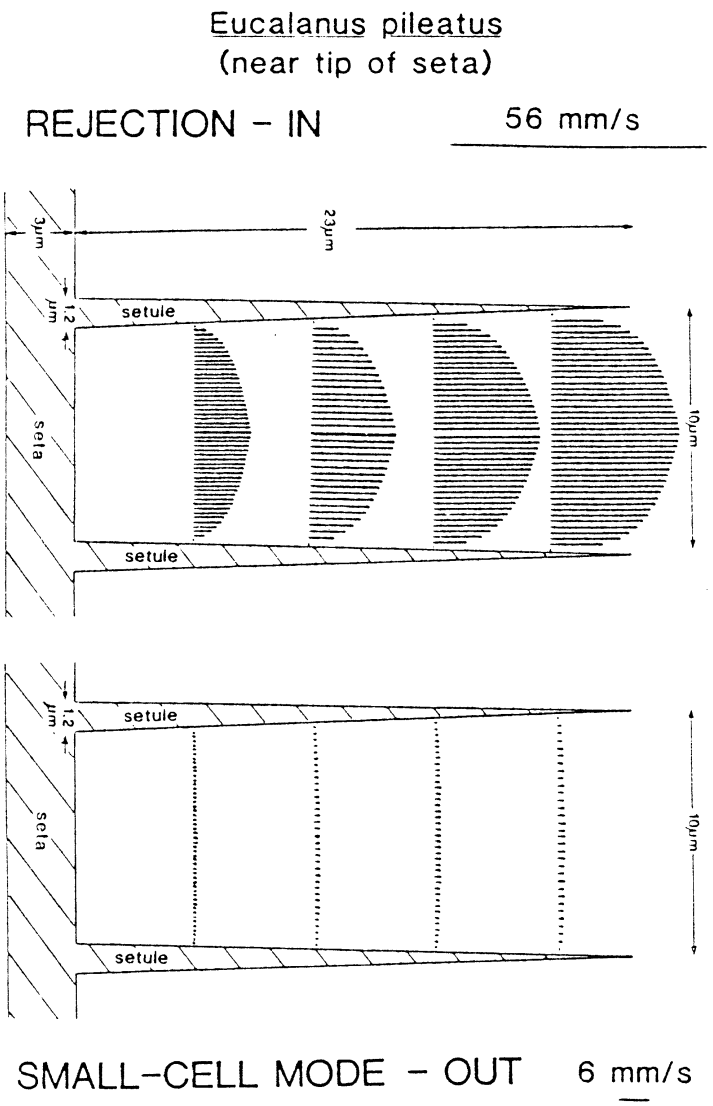

FIGURE 7. Diagram of longitudinal section of a portion of a seta of a M2 at position A (see Fig. 6) of a *Eucalanus pileatus* taken in the plane of one of the two rows of setules. Lines represent velocity vectors of water with respect to setules, but at right angles to the plane of the diagram; these vectors were calculated as described in Fig. 5. Upper diagram represents flow with respect to setules during the rapid inward sweep of a rejection motion (described in Ref. 3) when the gap between neighboring setae at position A is 50 μm. The lower diagram represents flow with respect to setules during the slow outward flap of the small-cell feeding mode (described in Ref. 24) when the gap between neighboring setae is only 23 μm. Line at upper right is free-stream velocity (at right angles to diagram) of water with respect to the seta during rejection motion, and line at lower right represents free-stream velocity with respect to the seta during small-cell mode. Leakiness values presented in text were calculated using profiles at a position 0.375 of the length of a setule from tip of setule.

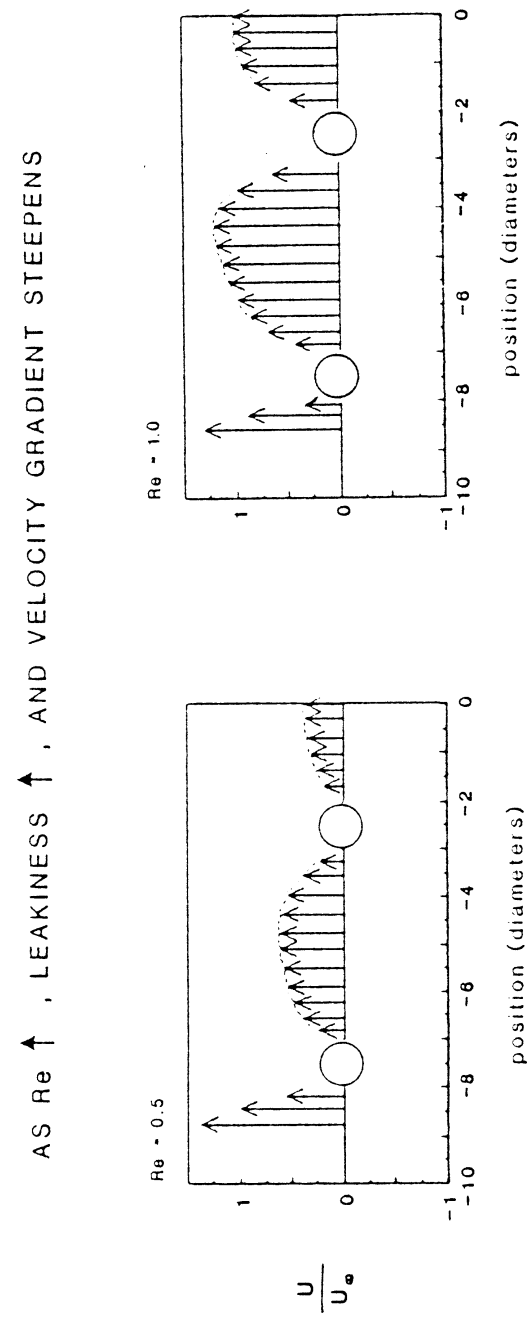
AS Re ↑ , LEAKINESS ↑ , AND VELOCITY GRADIENT STEEPENS
Re = 0.5
Re = 1.0
u/u∞
position (diameters)
position (diameters)
1
0
-1
-10
-8
-6
-4
-2
0

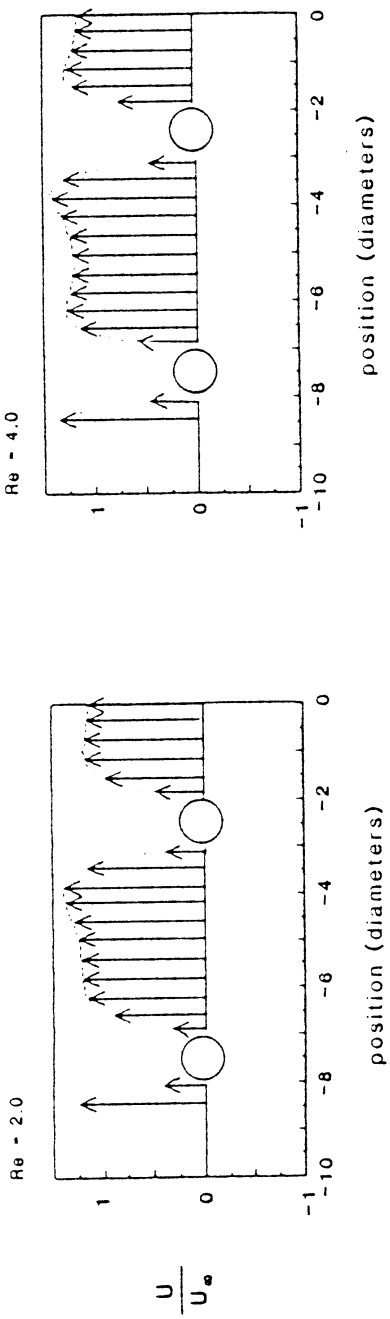

FIGURE 8. Velocity vectors (arrows) with respect to four cylinders in a row (gap/diameter = 4), calculated for various Reynolds numbers by Abdullah and Cheer (unpublished data) as described in text. Since flow fields are symmetric, only left half of row of cylinders is shown. Position (measured in cylinder diameters) is indicated on horizontal axis, and velocity (U) normalized to free-stream velocity (U_∞) is indicated on vertical axis.

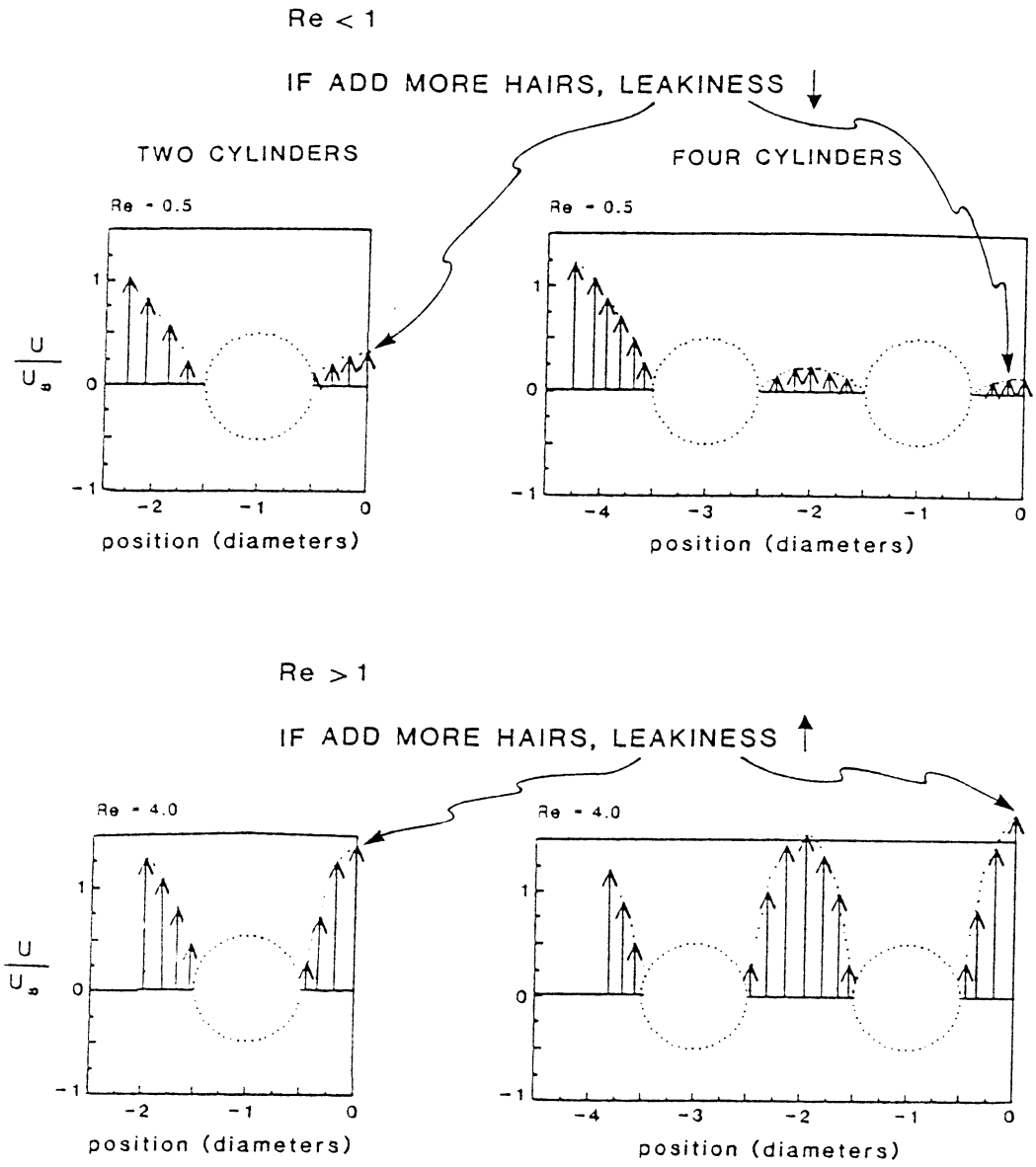

FIGURE 9. Velocity vectors with respect to two cylinders (graphs on the left) and four cylinders (graphs on the right) in a row (gap/diameter = 1), calculated for a Reynolds number of 0.5 (upper graphs) and 4.0 (lower graphs) by Abdullah and Cheer (unpublished data) as described in text. Since flow fields are symmetric, only left half of row of cylinders is shown. Position (measured in cylinder diameters) is indicated on horizontal axis, and velocity (U) normalized to free-stream velocity (U_∞) is indicated on vertical axis.

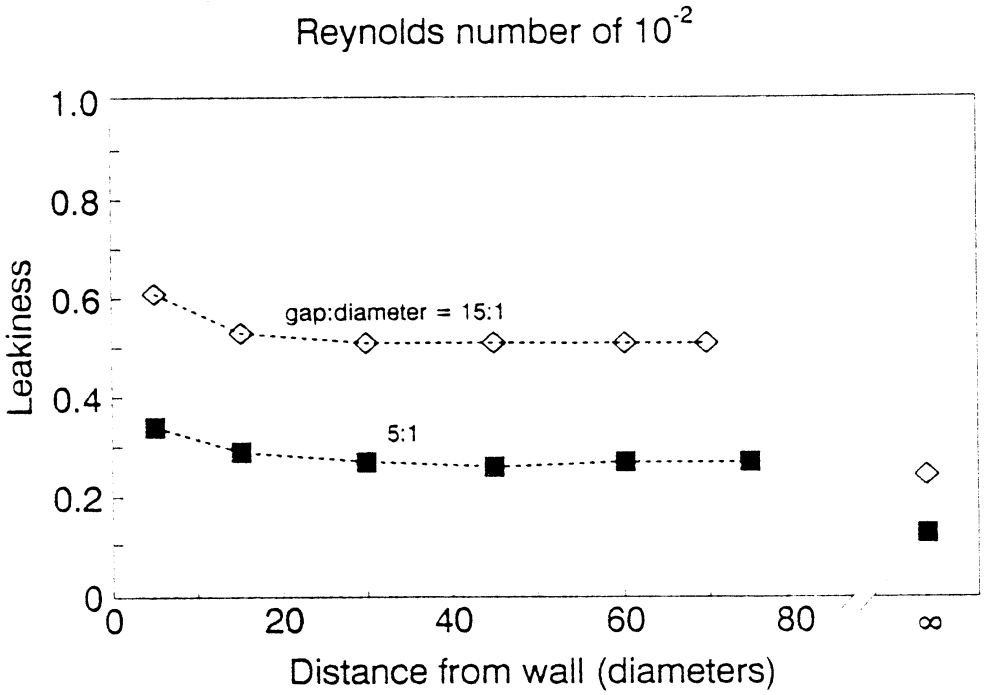

FIGURE 10. Leakiness (defined in text) of a pair of cylinders moving at Re = 10^{-2} at different distances from the side wall of a tank (Loudon, Best, and Koehl, unpublished data). Open diamonds represent data for a gap between cylinders that was 15 diameters in width, and black squares indicate data for a gap width of 5 diameters. Three duplicates of each measurement were made, and standard error bars were smaller than symbols indicating the mean value. Values for a distance of infinity were not measured, but rather were calculated using model of Cheer and Koehl (Ref. 8).

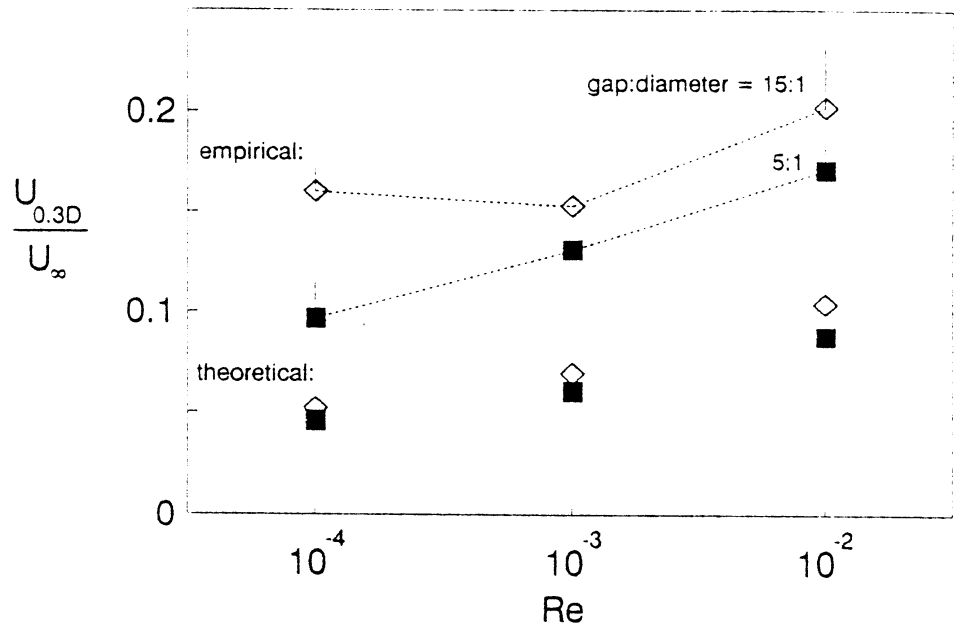

FIGURE 11. Steepness of velocity gradient in the gap between a pair of hairs moving at different Reynolds numbers. The measure of steepness of velocity gradient ($U_{0.3D}/U_\infty$) is the ratio of velocity of fluid relative to the hair at a distance of 0.3 diameter from surface of hair to free-stream velocity of fluid relative to the hairs. Open diamonds indicate values for a gap width of 15 diameters between hairs, and black squares indicate values for a gap width of 5 diameters. Data connected by dashed lines represent mean values of three duplicates of experiments using dynamically scaled physical models (error bars indicate one standard error) (Best, Loudon, and Koehl, unpublished data), whereas other values represent predictions calculated using model of Cheer and Koehl (Ref. 8).